1_C34

Measurements of Exhaled Airflow Velocity Via Human Coughs Using Particle Image Velocimetry (PIV)

Mengtao Han, PhD

Ryozo Ooka, PhD
Member ASHRAE

Hideki Kikumoto, PhD
Member ASHRAE

Wonseok Oh, PhD

Yunchen Bu

Shuyuan Hu

ABSTRACT

The sudden global outbreak of coronavirus diseases 2019 (COVID-19) has infected over seventy million people and resulted in over one million deaths by the end of 2020, posing a significant threat to human health. As potential carries of the novel coronavirus, exhaled airflow of infected individuals via coughs, are significant in virus transmission. This study measures human coughs' airflow velocity in a chamber filled with stage fog employing a particle image velocimetry (PIV) system. The purpose of this study is to examine and provide accurate boundary conditions for the prediction of the virus transmission routes using computational fluid dynamics (CFD) simulations. Sixty cough cases from ten healthy nonsmoking volunteers (five male and five female, averaged age of 29.3±4.0) are taken respectively, and ensemble-average operations are conducted to eliminate individual variations. Velocity distribution measurements are obtained in the vertical and horizontal planes around the mouth area. Temporal and spatial cough flow ensemble-averaged velocity profiles and standard deviations, cough duration time (CDT), peak velocity time (PVT), maximum cough velocities, and average spread angle of the cough jet are measured. Results show that the CDT of the cough airflow is 520–560 ms, and PVT is 20 ms. The male/ female averaged maximum velocity is 15.2/13.1 m/s, respectively. The average vertical/horizontal spread angle from the mouth is 15.3°/13.3° for males and 15.6°/14.2° for females, respectively. With the measurement data, it is possible to refine the initial boundary conditions of a simulated cough and model cough flows more accurately.

1. INTRODUCTION

The coronavirus diseases (COVID-19), globally broke out at the end of 2019, led to over 130 million infections and over 2.8 million deaths by March 2021, and became a serious global public health disaster. As a mediator of the coronavirus, the

Mengtao Han is an associate professor in School of Architecture and Urban Planning, Huazhong University of Science and Technology, Wuhan, China. **Ryozo Ooka** is a professor in Institute of Industrial Science, the University of Tokyo, Tokyo, Japan. **Hideki Kikumoto** is an associate professor in Institute of Industrial Science, the University of Tokyo, Tokyo, Japan. **Wonseok Oh** is a research fellow in Institute of Industrial Science, the University of Tokyo, Tokyo, Japan. **Yunchen Bu** is a graduate student in the Graduate School of Engineering, the University of Tokyo, Tokyo, Japan. **Shuyuan Hu** is a graduate student in the Graduate School of Engineering, the University of Tokyo, Tokyo, Japan.

airflow and the droplets/droplet nucleus from the infected people via coughs are considered important routes in the infection. Therefore, it is essential to clarify the coughs' airflow characteristics and the distribution of their initial velocity to study the droplets/droplet nucleus movement and the control of the virus infection. Accompanied by the development and application of computational fluid dynamics (CFD) technology, it becomes possible to simulate the droplet's motion via the human coughs in the architectural space. Therefore, it is crucial to clarify cough airflow characteristics and the distribution of initial velocity to validate the CFD simulation's accuracy and give the appropriate boundary condition.

Extensive studies have been carried out to characterize the flow behavior of cough and its initial velocity. Previous studies measured the cough flow rates varied with time and reported that flow rates ranged in 200-950 L/min (45-215 gals/min) with a mean peak of 300 L/min (68 gals/min), and peak flow rate by sex was of females and males were 750 and 1300 L/min (170 and 295 gals/min) of females and males, respectively (Mahajan et al. 1994; Singh et al. 1995). Several important indexes were defined to describe the characteristics of the cough airflow variation, such as the cough peak flow rate (CPFR), cough expiratory volume (CEV), and peak velocity time (PVT) (Gupta et al. 2009; Mahajan et al. 1994; Singh et al. 1995). In addition, several studies have made a great effort in the measurement or analysis of the initial cough velocity using a particle image velocimetry (PIV) and reported the maximum cough velocity could vary in the range of 1.5-28.8 m/s (4.1-94.6 ft/s) (Afshari et al. 2002; Chao et al. 2009; Dudalski et al. 2020; Marr et al. 2005; Wang et al. 2021; Zhu et al. 2006). In particular, Vansciver et al. 2011 measured the velocity profiles and maximum cough velocities during coughing for 29 subjects using PIV and obtained nondimensionalized velocity profiles. However, the profiles were aligned according to the peak velocity at each position and therefore lost turbulent information. Kwon et al. 2012 also measured and reported several instantaneous velocity vector fields of coughed airflow using PIV but did not provide detailed velocity profiles. Generally, there are mainly two disadvantages in the previous studies on cough airflow measurement. One is that the detailed distribution of temporal and spatial variation of initial velocity is still insufficient. The other is that the PIV's frequency is relatively low (usually less than 100 Hz). It may miss the critical characteristic of cough flow related to the time scale of the millisecond level. Another disadvantage for the low frequency is that the time and spatial resolution for measurement became rough, leading to the miss-capture of the tiny turbulence structure caused by the large initial velocity near the mouth.

Therefore, this study conducts cough airflow measurement utilizing a high-frequency PIV and yield detailed cough airflow characteristics and the velocity temporal and spatial distribution. Repeated cough cases from ten healthy young nonsmoking subjects are measured. Nondimensionalization and ensemble-average operations are carried out to eliminate individual variations and obtain general representative results. Overall cough airflow characteristics, such as peak velocity time, cough duration time, maximum velocity, and cough spread angle, were analyzed. Temporal and spatial distributions of cough airflow velocity around the mouth area are also obtained. This study provides the detailed validation database and probable boundary conditions for the subsequent CFD simulation of droplet propagation in the building environment.

2. EXPERIMENT METHODS

2.1. Settings of Semi-enclosed Chamber and PIV

A chamber and a PIV system were installed in a clean darkroom in the Institute of Industrial Science (IIS), the University of Tokyo. The room temperature and humidity were maintained at 24°C (75°F), 40-45% RH to imitate a general and representative indoor environment. The chamber with the size of $0.8 \times 0.5 \times 0.5m$ ($x \times y \times z, = 2.7 \times 1.8 \times 1.8\ ft$) was made of transparent acrylic boards (Figure 1a). The front panel is made of opaque boards to prevent subjects from being harmed by the laser, and there is a circular opening (diameter 0.05m) in the middle of the panel for coughs. The coordinate origin is defined in the middle of the opening (i.e., the center of the subjects' mouth). The x-, y-, and z-directions are defined as the airflow streamwise, spanwise, and vertical direction. The chamber was semi-enclosed to assure the air pressure balance during the coughing process. During the experiment, subjects were introduced to sit in front of the chamber and adjust to a proper height. The airflow exhaled from coughs was injected into the chamber which was full of stage fog (particle diameter is 1-10mm) through the circular opening. Table 1 lists the main parameters of the laser and PIV. In particular, the pulse interval of PIV was set at 1/2986s (i.e., the frequency was 2986 Hz) by balancing the maximum velocity and the capability of the camera lens. Vertical and horizontal distributions of the cough airflow velocities were measured (Figure 1b) through repeated cough cases, respectively. The velocity vector was analyzed by utilizing the adaptive correlation processing of two continuous images.

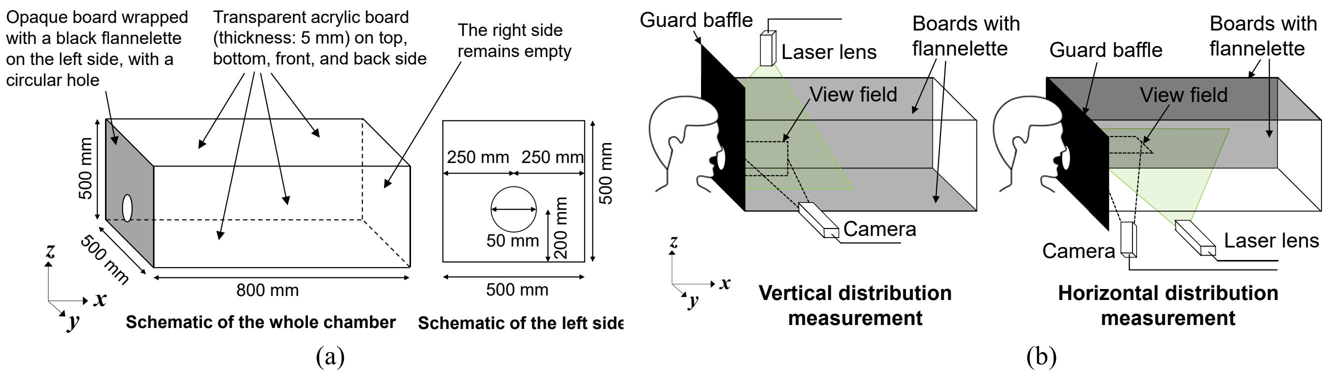

Figure 1 (a) Schematic of the chamber and (b) setups of the vertical and horizontal measurements using PIV.

Table 1. Parameters of PIV Setup

Illuminating Laser	Time between Laser Pulses [*s*]	Time between Recordings [*s*]	Size of View Field [*mm*; (*in*)]	Image Dimensions [*pixel*]	Interrogation Area [*pixel*]	Camera Lens
λ = 532 nm, Nd:YAG (neodymium-doped yttrium aluminum garnet.)	1/2986	1/2986	75 ×50 (2.95 × 1.97)	1200 × 800	32 ×32	Focal length: 15 mm, *f*: 2.8

2.2. Accuracy Examination of PIV

Ten-second time-averaged velocity was measured using a hotwire anemometer at several positions along with the jet flow and was regarded as benchmark data to examine the PIV's accuracy before the experiment. An air spray was utilized to imitate human mouths and continuously provided a stable jet flow.

Results depicted in Figure 2a shows that significant measurement error occurred when using the current PIV system because the cough airflow blew the fog particles away and led to an insufficient concentration of particles. We utilized a circular particle supplement tube at the opening (Figure 2b), in which small holes were set at an interval of about 1cm. Particles can be supplemented into the opening during the cough, and the outlet velocity of particles was less than 0.1 m/s to avoid impact on cough airflow. PIV's accuracy was improved when using the particle supplement tube and close to that of the hotwire anemometer.

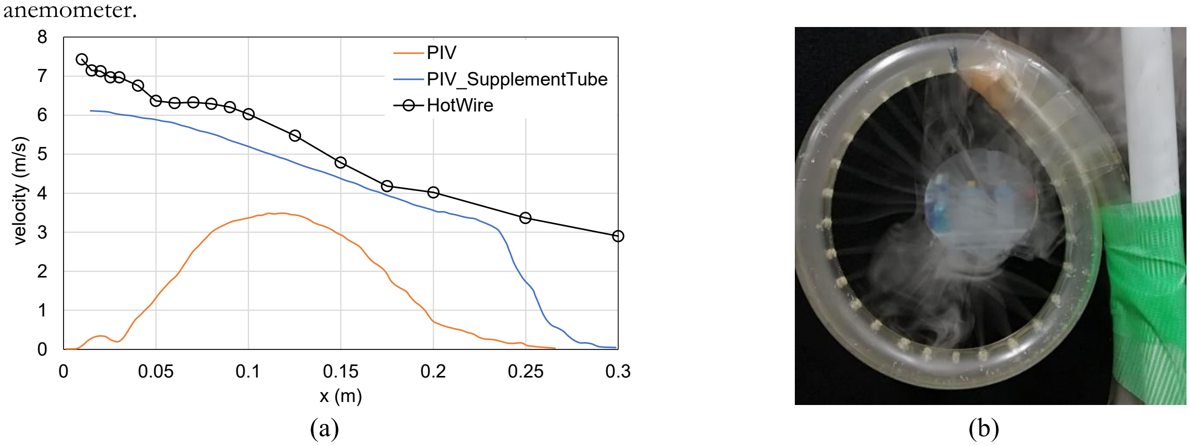

Figure 2 (a) Comparison of measurement results obtained by the hotwire anemometer, PIV, and PIV with the (b) particle supplement tube at the opening.

2.3. Experimental Subjects and Cough Cases

Ten healthy non-smoking young subjects (five males + five females) were employed, and six cough cases (three vertical measurements + three horizontal measurements) were measured for each subject. Table 2 tabulates the body characteristics of the subjects. Basic characteristics of cough airflow such as peak velocity time, cough duration time, peak velocity, and cough spread angle were examined from the measured data. Subsequently, the general distribution of airflow velocity was also analyzed, which individual variations were removed by conducting the nondimensionlization and ensemble-average operation.

Table 2. Basic Characteristics of Experimental Subjects

Male Subjects	Age [years]	Height [*m*; (*ft*)]	Mouth Width [*m*; (*ft*)]	Male Subjects	Age [years]	Height [*m*; (*ft*)]	Mouth Width [*m*; (*ft*)]
M1	33	1.61 (5.28)	0.045 (0.148)	F1	24	1.72 (5.64)	0.047 (0.154)
M2	26	1.65 (5.41)	0.052 (0.171)	F2	30	1.72 (5.64)	0.045 (0.148)
M3	37	1.73 (5.68)	0.048 (0.157)	F3	29	1.52 (4.99)	0.041 (0.135)
M4	26	1.75 (5.74)	0.053 (0.174)	F4	25	1.63 (5.35)	0.042 (0.138)
M5	31	1.88 (6.17)	0.037 (0.121)	F5	32	1.64 (5.38)	0.022 (0.072)
Average	30	1.72 (5.66)	0.047 (0.154)	Average	28	1.65 (5.41)	0.040 (0.131)

3. MEASUREMENT RESULTS AND DISCUSSIONS

3.1. Overall Cough Airflow Characteristics and Ensemble-average Operation

The overall cough airflow characteristics are first examined. Figure 3a shows the time variation of the maximum velocity at x/L_0 = 2.5 (L_0: mouth width) of one cough case. x/L_0 = 2.5 is approximately the center of the camera view field, where particle dilution and distorted perspectives less influenced the measurement data here, and the accuracy is higher than in other positions. The velocity peaked in a short time with a large acceleration and subsequently decayed gradually. This is the typical temporal variation for the maximum velocity of cough flow in all cases, similar to the cough airflow rate temporal variation reported by the previous study (Gupta et al. 2009). Referencing Gupta's research of airflow rate, we defined the peak velocity (PV) as the maximum velocity during the coughing process at a specific position (e.g., at x/L_0 = 2.5), peak velocity time (PVT) as the time that the velocity reached PV, and cough duration time (CDT) as the time that the whole cough process lasted, as shown in Figure 3a.

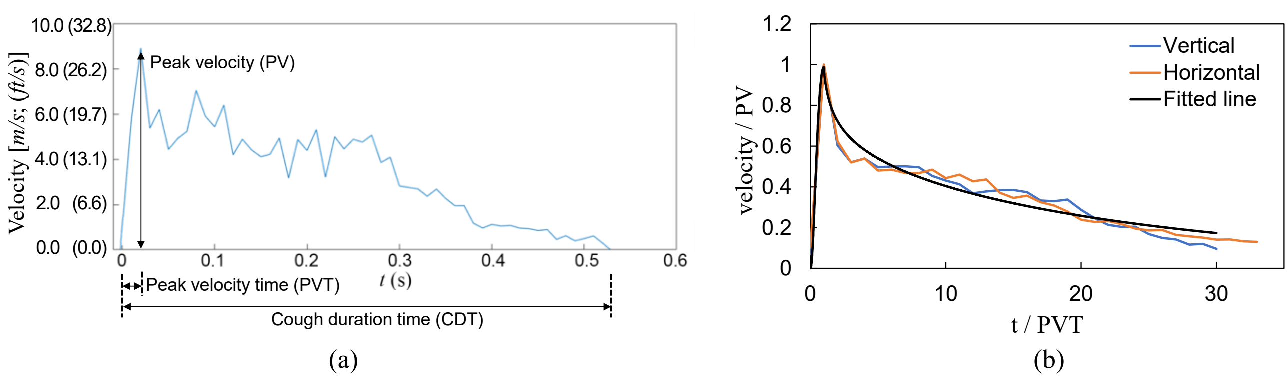

Figure 3 (a) Definitions of PV, PVT, and CDT. The background curve shows the maximum velocity temporal variation with time at x/L_0 = 2.5 of one cough case. (b) Ensemble-averaged maximum velocity temporal variation with time in vertical and horizontal directions of all cases with the fitted line at x/L_0 = 2.5.

Table 3 shows the statistics of PV, PVT, and CDT at x/L_0 = 2.5 in 60 times cough cases. Cough airflow reached PV at approximately 18-19 ms (PVT). The average PV of male/female was 11.8/10.3 m/s (38.7/33.8 ft/s). Both male and female CDT were approximately 500 ms. This indicates that the cough force was different by sex while their duration times were almost the same. It should be noticed that PV in Table 3 is the maximum velocity at x/L_0 = 2.5 while not the maximum of the whole measurement area. Table 3 also reports the maximum velocity in the whole measurement domain during the coughing process, which agreed well with a previous study (Kwon et al. 2012).

Table 3. Variation Range of PV, PVT, and CDT of All Cases and Their Averaged Values (Avg.), Standard Deviation Values (SD) at $x/L_0 = 2.5$

Sex	PV [*m/s*; (*ft/s*)] Variation range	PV Avg. / SD	PVT [*ms*] Variation range	PVT Avg. / SD	CDT [*ms*] Variation range	CDT Avg. / SD	Max. Cough Velocity [*m/s*; (*ft/s*)] Variation range	Max. Cough Velocity Avg. / SD	Max. Cough Velocity Kwon et al. 2012
Male	6.4–18.6 (21.0–61.0)	11.8 / 3.3 (38.7 / 10.8)	8–35	19 / 7	277–904	564 / 158	7.3–20.9 (24.0–68.6)	15.2 / 3.3 (50.0 / 10.8)	15.3 (50.2)
Female	5.0–15.7 (16.4–51.5)	10.3 / 3.0 (33.8 / 9.8)	8–39	18 / 6	343–825	526 / 131	8.2–19.1 (26.9–62.7)	13.1 / 3.1 (43.0 / 10.2)	10.6 (34.8)

To obtain general temporal maximum velocity variation curves, all cough cases were nondimensionalized using their own PVs, PVTs, and subjects' mouth widths for velocities, times, and lengths. Subsequently, all cases were ensemble-averaged according to vertical and horizontal directions, as shown in Figure 3b. The vertical and horizontal curves agreed well, implying that cough airflow's vertical and horizontal components owned similar characteristics. These curves were similar to the airflow rate variation curve reported by Gupta, which followed the gamma probability distribution. Therefore, we also fitted these curves utilizing the gamma probability distribution function $\Gamma(\cdot)$, as shown in Equation 1. Here, t represents the time, and τ is the nondimensional time. In the acceleration process ($\tau < 1.0$), Gupta's equation was directly adopted, and the same shape was applied in the decaying process ($\tau \geq 1.0$). Therefore, the temporal variation of the maximum velocity followed the gamma probability distribution function well.

$$\begin{array}{c}\text{maximum velocity} \\ (\text{at } x/L_0 = 2.5)\end{array} = \begin{cases} \dfrac{a_1 \tau^{b_1 - 1} \exp\left(\dfrac{-\tau}{c_1}\right)}{\Gamma(b_1) c_1^{b_1}} & \text{for } \tau < 1.0 \\[2ex] \dfrac{a_2 (\tau + d_2)^{b_2 - 1} \exp\left(\dfrac{-(\tau + d_2)}{c_2}\right)}{\Gamma(b_2) c_2^{b_2}} & \text{for } \tau \geq 1.0 \end{cases} \tag{1}$$

$$\tau = \frac{t}{PVT}, a_1 = 1.680, b_1 = 3.338, c_1 = 0.428, a_2 = 15.32, b_2 = 0.8435, c_2 = 29.95, d_2 = -0.769.$$

3.2. Temporal and Spatial Distribution of Cough Airflow Ensemble-averaged Velocity

All 60 cough cases were divided into vertical and horizontal groups. The ensemble-average operation was performed after their nondimensionalizations for each group to obtain the general and representative temporal and spatial velocity distribution. It should be noticed that PIV is only capable of measuring the velocity in a two-dimensional plane, and thus the result of the vertical velocity distribution is $\langle\sqrt{u_x^2 + u_z^2}\rangle$, lacking in the spanwise component. The horizontal distribution is $\langle\sqrt{u_x^2 + u_y^2}\rangle$ and lacks in the vertical component. Here, the bracket $\langle\cdot\rangle$ represents the ensemble-average operation.

The spatial distribution of ensemble-averaged velocity and its standard deviation at the time of t/PVT = 1.0, 5.0, and 10.0 are shown in Figure 4. The velocity decayed with the increase of *x*-distance due to the airflow diffusion and the energy decaying. In both vertical and horizontal distributions, the spatial range of the airflow tended to spread gradually with an increase of *x*-distance, indicating that the airflow from the mouth had a spread angle, which will be discussed in Section 3.3

Figure 5 shows the temporal distribution of averaged velocity and standard deviation at the position of x/L_0 = 1.0 and 2.5. At all positions, the velocity rapidly increased and subsequently gradually decayed after it peaked. This is in good agreement with the tendency shown in Figure 3. In contrast to Figure 4, the spatial range of velocity shown in Figure 5 generally constant with time development. This indicates that the airflow spread with the increase in the distance, but the shape was generally constant over time. Thus, the cough airflow had partial jet flow characteristics, which is consistent with previous reports (Chao et al. 2009; Gupta et al. 2009; Marr et al. 2005; Vansciver et al. 2011).

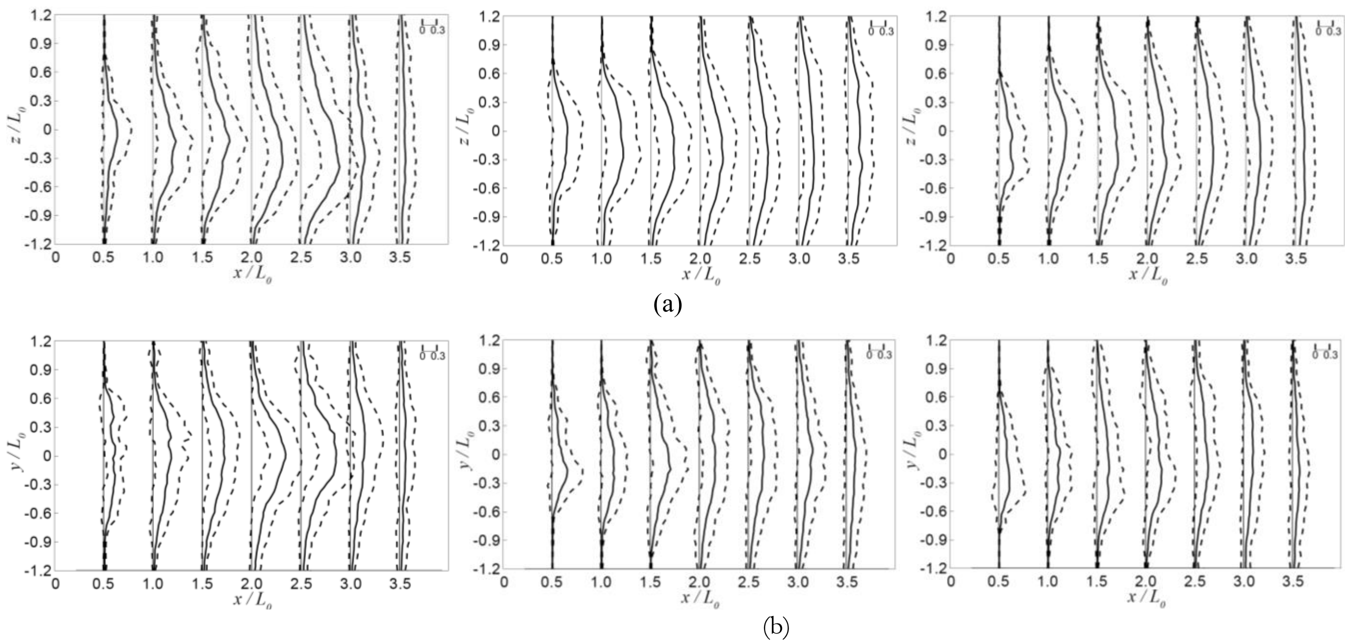

Figure 4 (a) Vertical and (b) horizontal spatial distribution of 60-cases ensemble-averaged velocity. Solid line: averaged velocity; dashed line: ±1 standard deviation (confidence interval: 68.3%). The left, middle, and right figures represent the time of t/PVT = 1.0, 5.0, and 10.0.

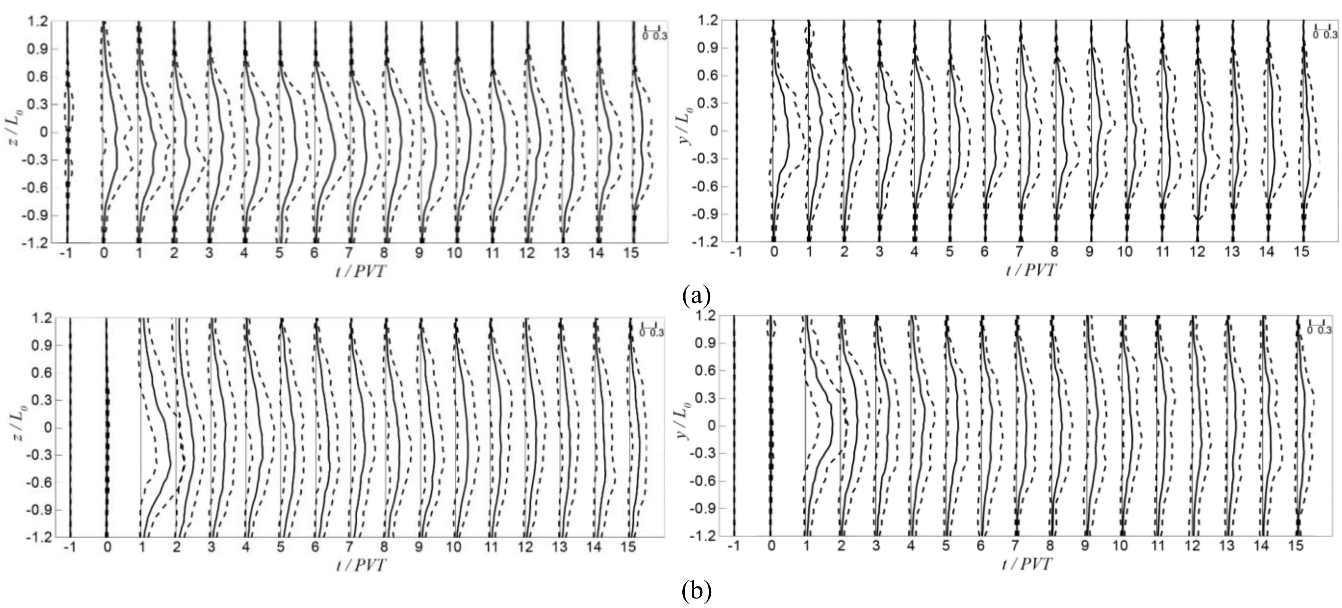

Figure 5 Temporal distribution of 60-cases ensemble-averaged velocity at positions of (a) x/L_0 = 1.0 and (b) x/L_0 = 2.5. Solid line: averaged velocity; dashed line: ±1 standard deviation (confidence interval: 68.3%). The left and right figures represent the vertical and horizontal distribution, respectively.

3.3. Cough Spread Angles

Generally, the cough airflow exhaled from the mouth has an angle that spreads like the jet. This section analyzes the vertical cough spread angle θ_V and the horizontal cough spread angle θ_H. It is most important to determine the edges of the upper/lower sides and left/right boundaries of cough airflow to yield the spread angles. In the previous studies (Gupta et al. 2009), these boundaries were usually determined by directly drawing the edge lines in the raw particle images. This method is simple and intuitive but has a large error.

This study imitates the definition of the velocity boundary layer in fluid mechanics and introduces a more quantitative method for determining the cough airflow boundaries (Figure 6). Considering the jet characteristics of cough airflow, the boundary points were defined as the points that the velocity was 1% of the central maximum velocity (i.e., the velocity was 99% attenuated) in the vertical and horizontal positions. Subsequently, the boundary edges were fitted from all the boundary points using the least square method. The angle between the boundary edges is the airflow spread angle.

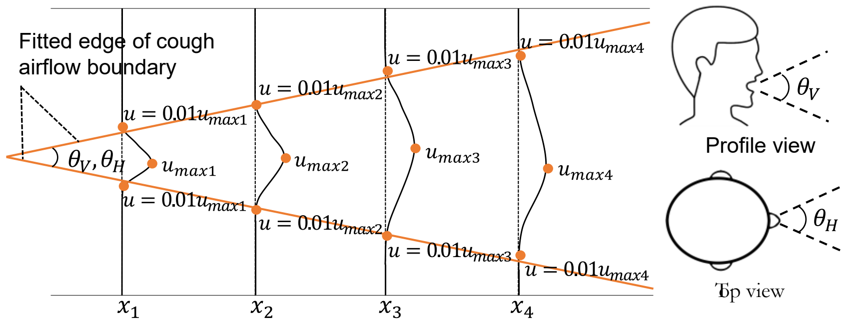

Figure 6 Schematic of determination of cough airflow boundary edge and definition of cough spread angles θ_V, θ_H. Black solid curves represent velocity distribution at several positions; orange points represent feature points (maximum velocity and 1% of maximum velocity); solid orange lines were edge of cough airflow boundary fitted by feature points.

Table 4 shows the ensemble-averaged vertical spread angle θ_V, and horizontal spread angle θ_H, and compared with other studies. θ_V varied in the range of 4–27°and θ_H varied in the range of 4–31°. The mean value of males/females was θ_V = 15.3 °/ 15.6 °and θ_H = 13.3 °/ 14.2 °. The differences by sex were small. The spread angle obtained by this study is significantly different from that of Gupta's study. In addition to the difference in determining the airflow boundary, several experimental conditions were also different in both studies. For example, case numbers were different (this study 15 vs. Gupta 5), and head situations of subjects were also different (heads were fixed using auxiliary devices in Gupta's experiment while were free but stabilized much as possible in this study). These differences may cause a discrepancy in the cough flow spread angle.

Table 4. Vertical θ_V and Horizontal θ_H of Cough Spread Angles

Items	θ_V (°)	θ_H (°)
Averaged value of male subjects	15.3	13.3
Averaged value of female subjects	15.6	14.2
All averaged value of all subjects	15.5	13.8
Gupta et al. (Gupta et al. 2009)	25	-

4. CONCLUSIONS

In this study, 60 cough cases from 10 healthy young subjects were measured using a high-frequency PIV to analyze the cough airflow characteristics, such as maximum velocity, PV, PVT, CDT, and spread angles. The detailed temporal and spatial distribution of airflow velocity in vertical and horizontal directions were also obtained.

The maximum coughing velocity for females was weaker than that for males, but their PVT or CDT was similar, implying that their cough duration time was almost the same. In addition, the nondimensional velocity distribution for males and females agreed well in both vertical and horizontal directions, indicating that their cough airflows own similar characteristics. The temporal variations of maximum velocity at x/L_0 = 2.5 can be defined as a combination of gamma-probability-distribution functions. The cough spread angles were analyzed by determining the cough airflow boundaries as the position where the velocity decayed to 1% of the maximum value at the airflow center in every vertical or horizontal direction. The cough spread angles of males and females were also almost the same. The vertical and horizontal spread angles were similar, implying that the initial cough airflow exhaled from the mouth was promising to be modeled as a cone. This should be further studied.

This study's PIV data provides a basis to understand human cough characteristics and dataset and boundary conditions for CFD validation to model cough airflows in the future. The mouth width, maximum velocity, velocity distribution, CDT, and cough spread angles reported in the study can be the possible boundary conditions for cough airflow CFD simulation. In addition, PV and PVT can provide the nondimensionalization parameters for simulation results. These will be validated in the subsequent study on CFD simulation of the droplets propagation via cough airflow.

NOMENCLATURE

L_0 = mouth length
θ_V = vertical cough spread angle
θ_H = horizontal cough spread angle
$\langle\cdot\rangle$ = ensemble-averaged value
x,y,z = streamwise, spanwise, and vertical components of the spatial coordinate, respectively
u_x,u_y,u_z = components of instantaneous velocity in the *x*, *y*, and *z* directions, respectively

REFERENCES

Afshari, A., S. Azadi, T. Ebeling, A. Badeau, W. T. Goldsmith, K. C. Weber, and D. G. Frazer. 2002. Evaluation of cough using digital particle image velocimetry. In *Proceedings of the Second Joint 24th Annual Conference and the Annual Fall Meeting of the Biomedical Engineering Society] [Engineering in Medicine and Biology* (Vol. 2, pp. 975–976). IEEE.

Chao, C. Y. H., M. P. Wan, L. Morawska, G. R. Johnson, Z. D. Ristovski, M. Hargreaves, K. Mengersen, S. Corbett, Y. Li, X. Xie, and D. Katoshevski. 2009. Characterization of expiration air jets and droplet size distributions immediately at the mouth opening. *Journal of Aerosol Science*, *40*(2):122–133.

Dudalski, N., A. Mohamed, S. Mubareka, R. Bi, C. Zhang, and E. Savory. 2020. Experimental investigation of far-field human cough airflows from healthy and influenza-infected subjects. *Indoor Air*, *30*(5):966–977.

Gupta, J. K., C. H. Lin, and Q. Chen. 2009. Flow dynamics and characterization of a cough. *Indoor Air*, *19*(6):517–525. Kwon, S. B., J. Park, J. Jang, Y. Cho, D. S. Park, C. Kim, G. N. Bae, and A. Jang. 2012. Study on the initial velocity distribution of exhaled air from coughing and speaking. *Chemosphere*, *87*(11):1260–1264.

Mahajan, P., P. Singh, G. Murty, and A. Aitkenhead. 1994. Relationship between expired lung volume, peak flow rate and peak velocity time during a voluntary cough manoeuvre. *British Journal of Anaesthesia*, *72*:298–301.

Marr, D., H. Higuchi, T. Khan, J. Zhang, and M. Glauser. 2005. On Particle Image Velocimetry (PIV) measurements in the breathing zone of a thermal breathing manikin. *ASHRAE Transactions*, *111 PART 2*:299–305.

Singh, P., R. P. Mahajan, G. E. Murty, and A. R. Aitkenhead. 1995. Relationship of peak flow rate and peak velocity time during voluntary coughing. *British Journal of Anaesthesia*, *74*(6):714–6.

Vansciver, M., S. Miller, and J. Hertzberg. 2011. Particle image velocimetry of human cough. *Aerosol Science and Technology*, *45*(3):415–422.

Wang, C. T., S. C. Fu, and C. Y. H. Chao. 2021. Short-range bioaerosol deposition and recovery of viable viruses and bacteria on surfaces from a cough and implications for respiratory disease transmission. *Aerosol Science and Technology*, *55*(2):215–230.

Zhu, S., S. Kato, and J.-H. Yang. 2006. Study on transport characteristics of saliva droplets produced by coughing in a calm indoor environment. *Building and Environment*, *41*(12):1691–1702.